

Electronic Supplementary Information: Computational Simulations Determining Disulfonic Stilbene Derivatives Biodisponibility Within Human Serum Albumin

Titouan Jaunet-Lahary,^a Daniel P. Vercauteren,^{a,b} Fabrice Fleury^c and Adèle D. Laurent^{*a}

^a Laboratoire CEISAM - UMR CNRS 6230, Université de Nantes,
2 Rue de la Houssinière, BP 92208, 44322 Nantes Cedex 3, France.

^b Unité de Chimie Physique Théorique et Structurale,
Namur Medicine & Drug Innovation Center (NAMEDEC),
University of Namur, Rue de Bruxelles 61, B-5000 Namur, Belgium.

^c Laboratoire UFIP - UMR CNRS 6286, Université de Nantes,
2 Rue de la Houssinière, BP 92208, 44322 Nantes Cedex 3, France.

E-mail: Adele.Laurent@univ-nantes.fr

Contents

1	Docking validation	2
1.1	Molecular docking: poses and docking scores	2
2	Protein C_α and binding site RMSD	5
3	IB binding site	7
3.1	DADS ligand	7
3.2	DNDS ligand	9
3.3	DATDS ligand	9
4	IIA binding site	11
4.1	DADS ligand	11
4.2	DNDS ligand	14
4.3	DATDS ligand	16
5	IIAIB binding site	17
5.1	DADS ligand	17
5.2	DNDS ligand	17
5.3	DATDS ligand	18

6 IIIA binding site	19
6.1 DADS ligand	19
6.2 DNDS ligand	21
6.3 DATDS ligand	22

1 Docking validation

To validate our docking protocol, we considered existing drug-HSA complexes from PDB, 2VUE (HSA-bilirubin)¹, 2BXD (HSA-warfarin)² and 2BXG (HSA-ibuprofen)², and re-docked the drug within its binding site. In each case, we got the same orientation and position than the crystallographic structure. The superimposition of the ligand best pose and the X-ray structure are presented in Figure 1.

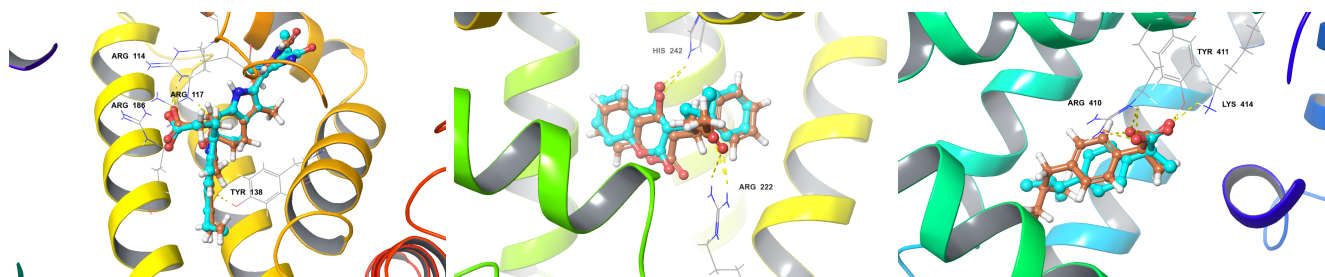


Figure ESI- 1 Left to right, best poses obtained after the molecular docking for bilirubin, warfarin and Ibuprofen, respectively. In orange (blue), the ligand obtained from molecular docking (from the crystallographic structure).

1.1 Molecular docking: poses and docking scores

The docking calculations of DADS generated 53 different poses distributed into 3 main clusters of 27, 8 and 18 poses when looking at the RMSD matrix. The two first clusters are clearly superimposed in Figure 2.

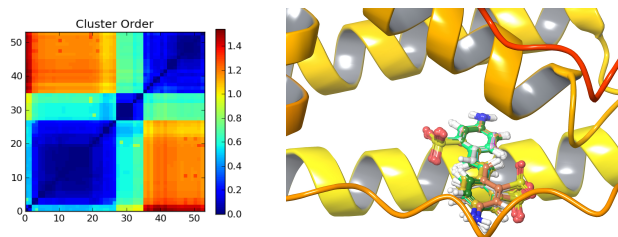


Figure ESI- 2 Left, RMSD matrix (Å) of the various DADS docking poses within the IB binding site of the ASH. Right, superimposition of the 35 poses from the first and second cluster of the DADS²⁻ docking calculations.

Docking score/Glide energy (in kcal/mol) for each ligand in each binding site are given found in Table 2.

Energy of each docking pose as computed with the CHARMM force field (in kcal/mol) to be compare to Table ESI-1. 2.

Table ESI- 1 Docking score/Glide energy (in kcal/mol) for each ligand in each binding site.

	IB	IIA	IIAIIB	IIIA
DADS-HSA	-7,54/-62.08	-7.13/-61.25 (out) -7.23/-51.69 (in)	-6.09/-61.91	-5.01/-64.21
DATDS-HSA	-6.11/-65.01	-7.17/-76.50 (out)	-4.73/-86.91	-6.35/-72,70
DNDS-HSA	-6.44/-60.91	-7.58/-73.76 (in)	-5,85/-68.79	-5.28/-54.15

Table ESI- 2 Energy of each docking pose as computed with the CHARMM force field (in kcal/mol).

	IB	IIA	IIAIIB	IIIA
DADS-HSA	2613.3	3465.0(out) -2568.0 (in)	-2928.0	-2947.7
DNDS-HSA	-2648.5	-3262.4(in)	-2642.1	-2947.7
DATDS-HSA	-2450.6	-3475.7 (out)	-3015.45	2983.1

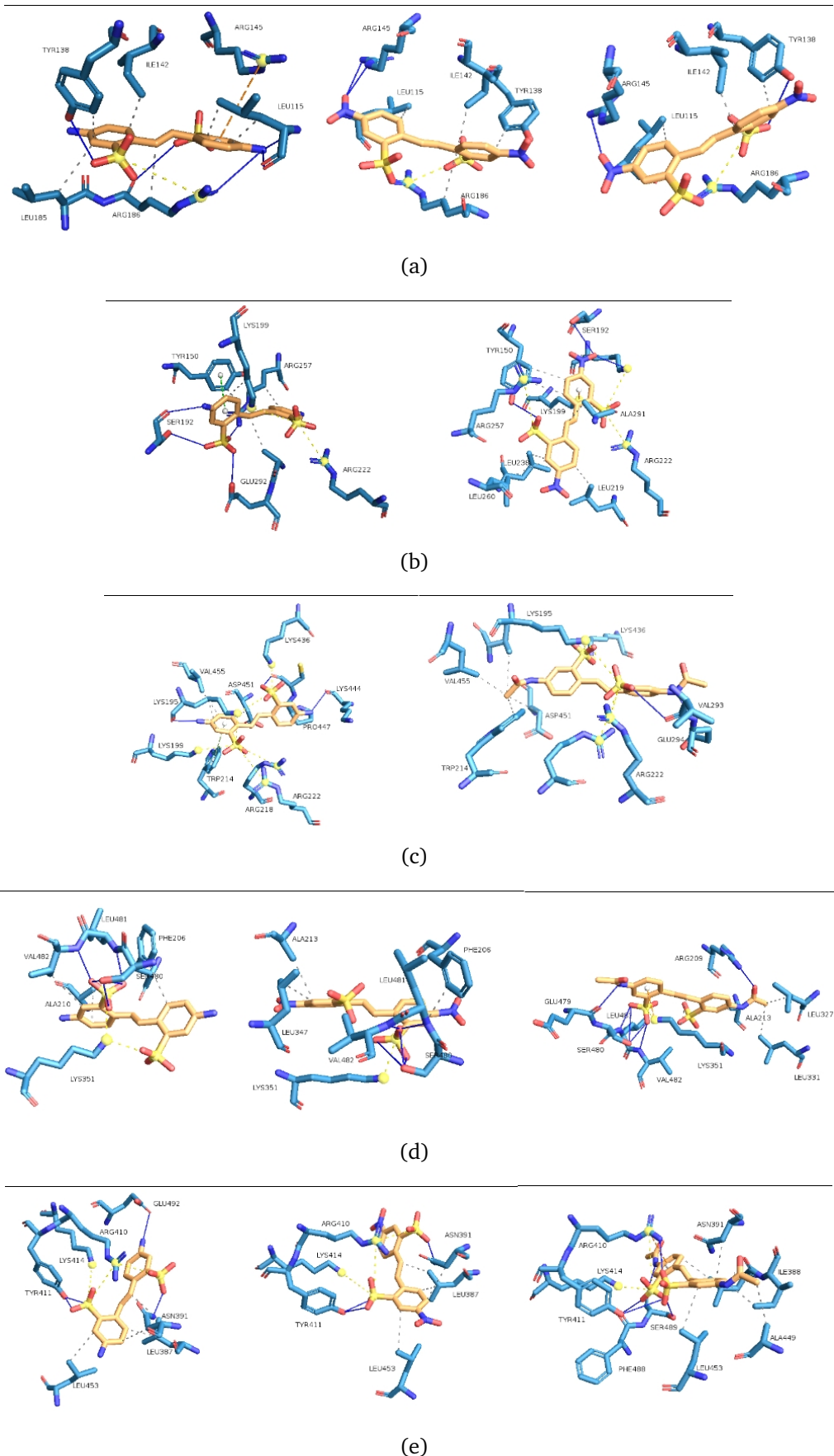


Figure ESI- 3 Left to right are respectively the selected docking pose of DADS, DNDS and DATDS in (a) IB site, (b) IIA (in) site, (c) IIA (out) site, (d) IIAIIB site, (e) IIIA site of HSA.

2 Protein C_α and binding site RMSD

RMSD of the protein and each binding site with each ligand were computed in order to evaluate the MD convergence (Figures 4 and 5).

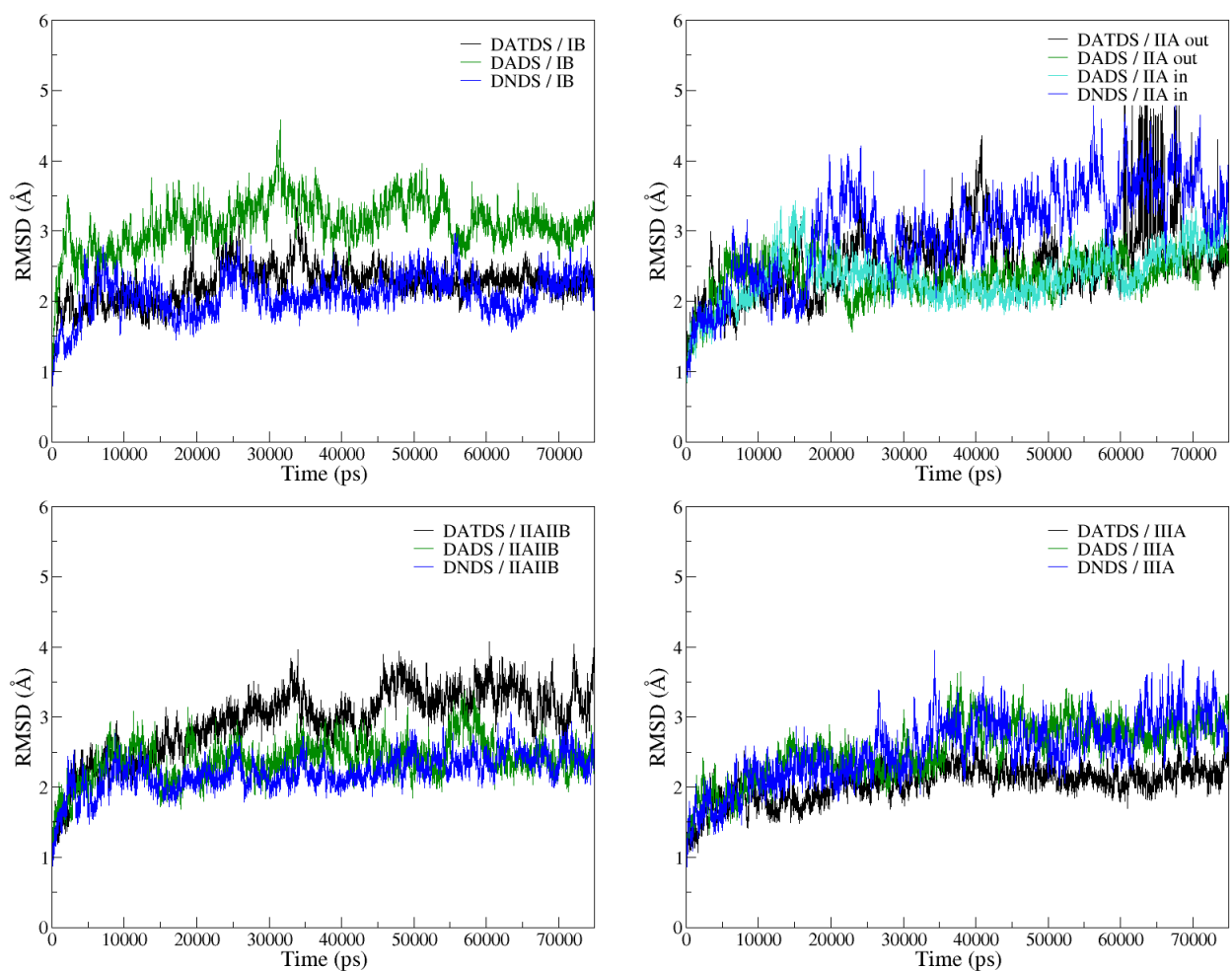


Figure ESI- 4 Alpha carbon RMSD of the protein for each ligand embedded into the investigated binding sites from MD simulations.

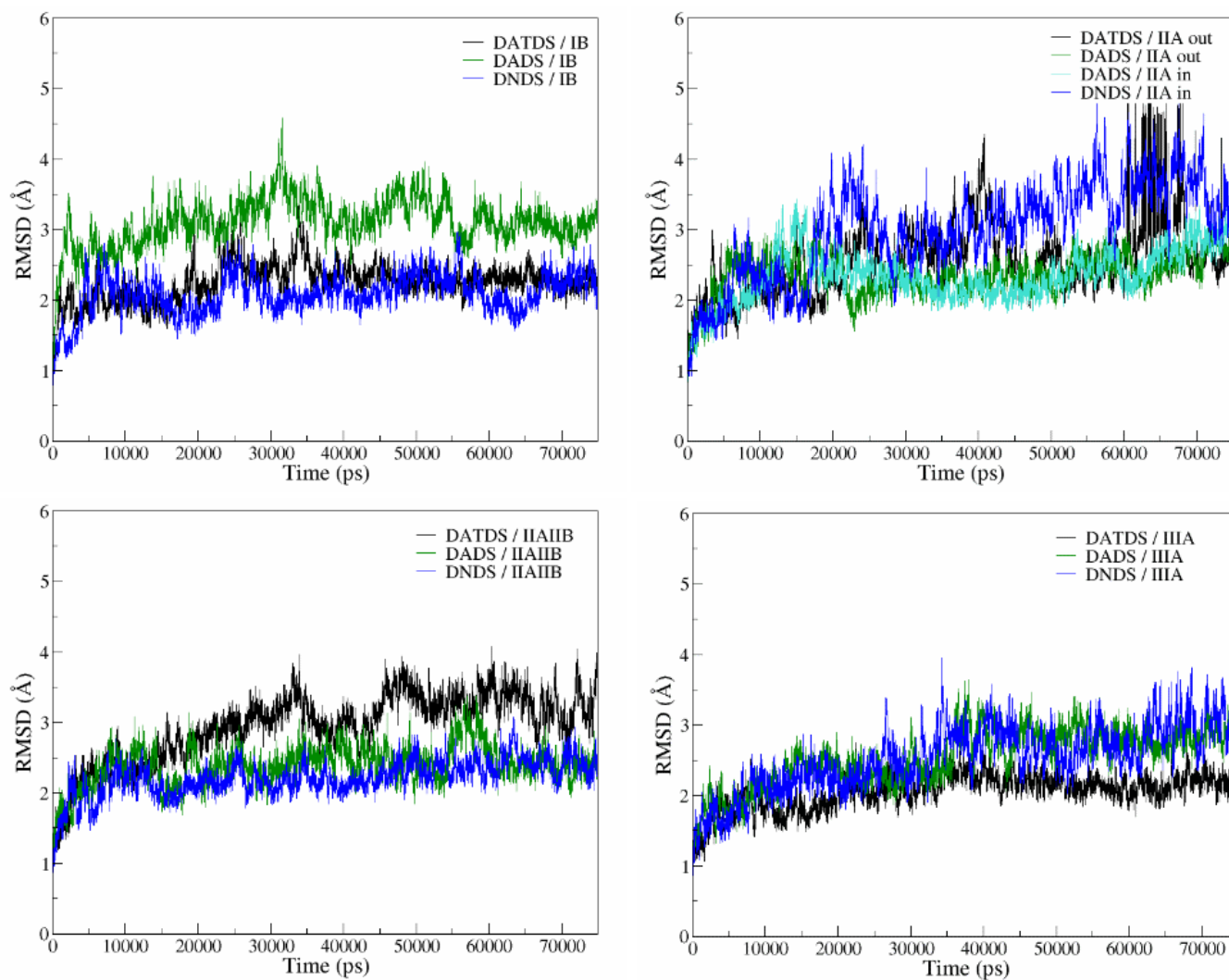


Figure ESI- 5 RMSD matrix (Å) of the various ligands within each binding site from MD simulations.

3 IB binding site

3.1 DADS ligand

RMSF are depicted in Figure 6 for the apo and holoHSA (ligand within IB site) systems. The presence of the ligand induces a slightly higher fluctuation of one of the alpha helices compared to the apoHSA. Such a difference is not impacting on the ligand binding.

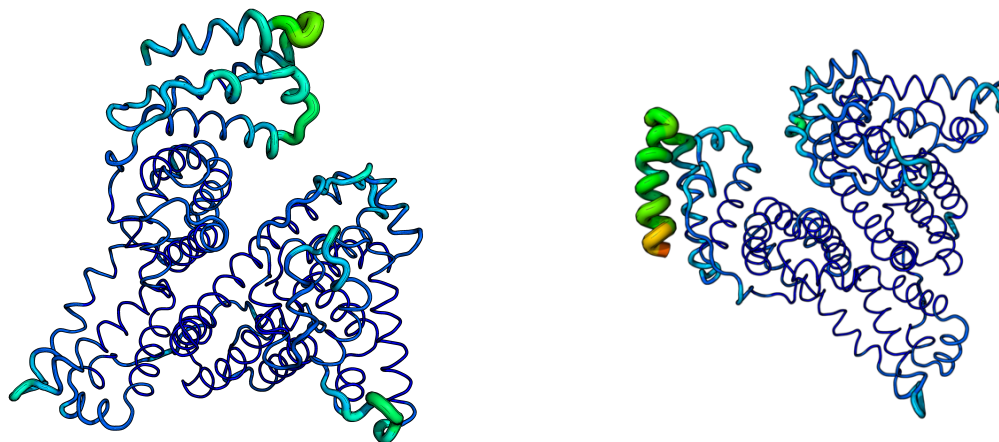


Figure ESI- 6 RMSF per residue of the apoHSA (left) and DADS embedded into IB site systems (right) calculated from the 75 ns MD simulations. Red and blue depict regions of higher and lower fluctuations, respectively.

Between 7 and 10 ns, Arg186 is flipped, breaking its interaction with DADS and leaving some space to the ligand to deeper enter in the binding pocket (Figure 7, 10 ns). Such movements induce the disruption of DADS specific interactions with Tyr138 and Lys190 while Arg117 is again forming a salt bridge with the same SO_3^- entity of DADS as in the docking pose. The interactions between DATDS and Arg117 of the IB binding site of HSA is depicted in Figure 7.

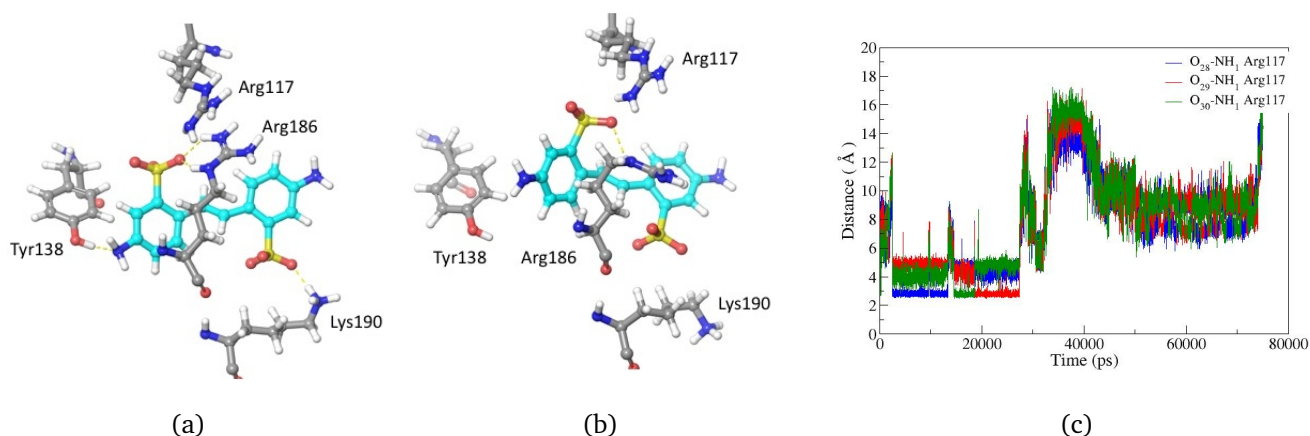
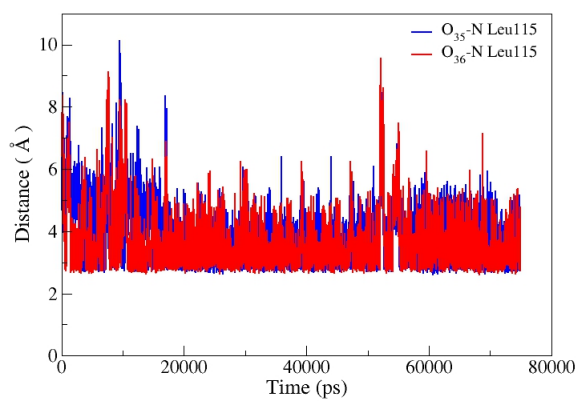
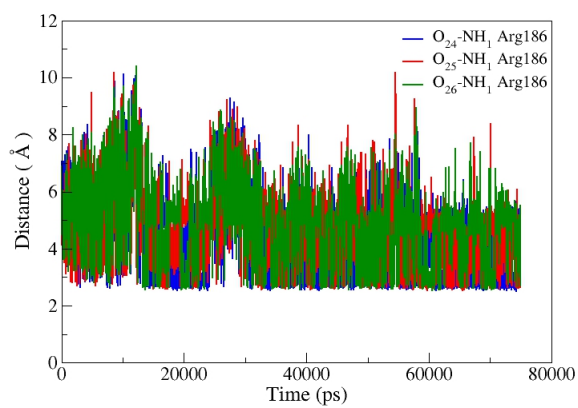


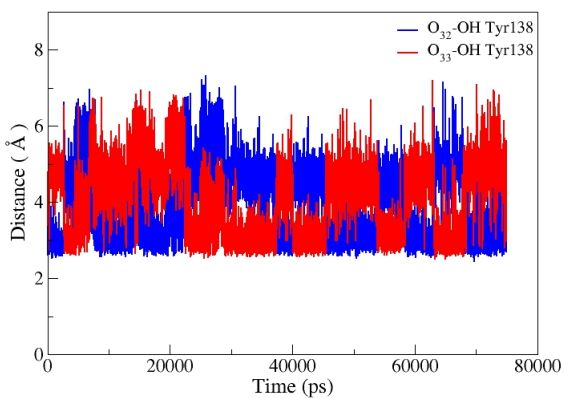
Figure ESI- 7 Snapshots showing the environmental changes of DADS in the IB pocket of HSA as obtained from the MD simulation at 5 ns (a) and 10 ns (b). (c) Distances between the oxygen atoms of the DATDS sulfonate group and nitrogen of Arg117 of HSA obtained from the MD simulations.



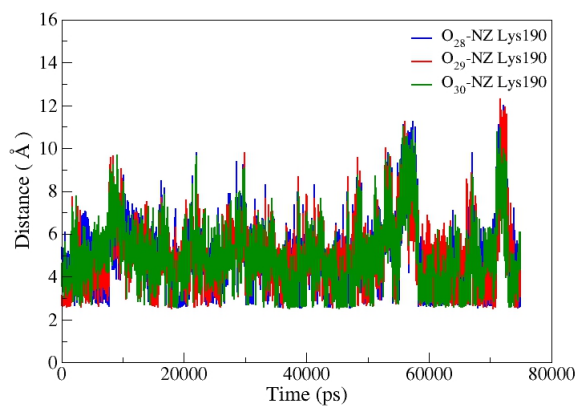
(a)



(b)



(c)

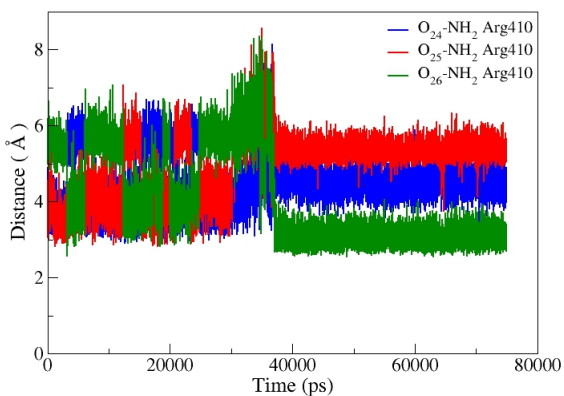


(d)

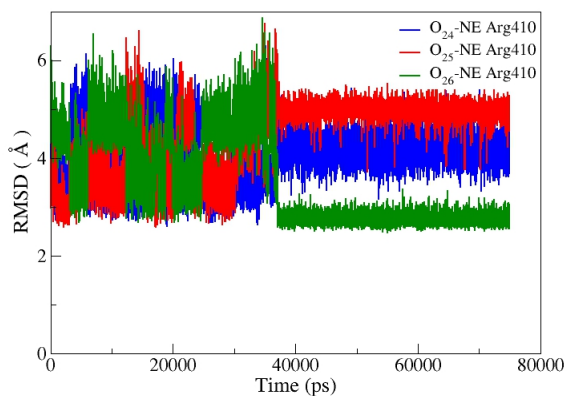
Figure ESI- 8 Distances between the oxygen atoms of the DNDS sulfonate groups and (a) oxygen of Leu115 , (b) oxygen of Arg186, (c) oxygen of Tyr138, (d) nitrogen of Lys190 of HSA obtained from the MD simulations.

3.2 DNDS ligand

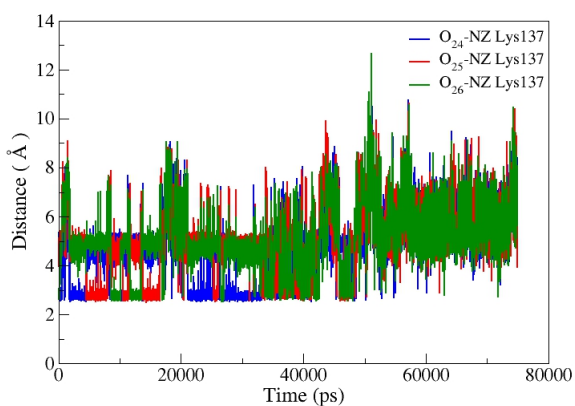
3.3 DATDS ligand



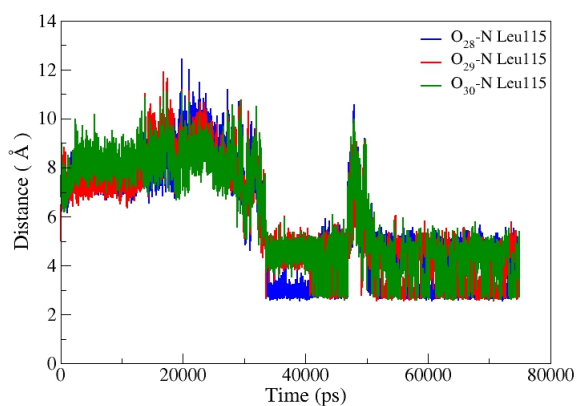
(a)



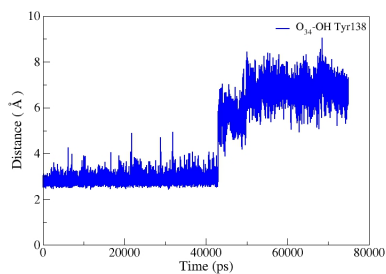
(b)



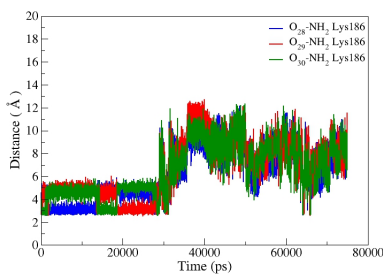
(c)



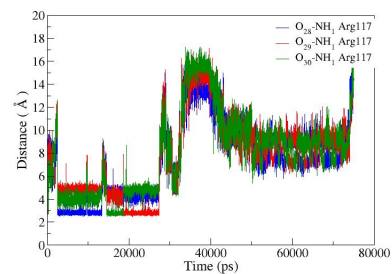
(d)



(e)



(f)



(g)

Figure ESI- 9 Distances between the oxygen atoms of the DATDS sulfonate groups and (a) and (b) backbone and sidechain nitrogen atoms of Arg410, (c) oxygen of Lys137, (d) backbone oxygen of Leu115, (e) oxygen of Tyr138, (f) oxygen of Arg186, (g) oxygen of Arg117 of HSA obtained from the MD simulations.

4 IIA binding site

4.1 DADS ligand

Molecular docking led to 62 poses distributed in two main clusters. The RMSD matrix obtained after the clustering step of the poses is shown in Figure 10. RMSD values are going up to 2.25 Å.

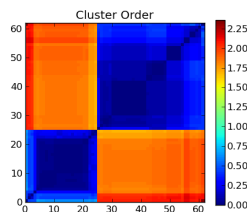


Figure ESI- 10 RMSD matrix (Å) of the various DADS docking poses within the IIA binding site of the HSA protein.

Concerning the DADS when located inside the warfarin binding pocket, the global structure of HSA is not modified by the presence of the ligand. The RMSD values of α -carbon of the apo and holo HSA (DADS inside the binding pocket) proteins obtained from the MD simulation and the RMSF values depicted in Figure 11 clearly show that the DADS binding in this pocket does not affect the global structure of HSA (cfr. comparison of the RMSF in Figure 11). At 34 ns, Lys195 is approaching one sulfonate group, leading to a movement of the Arg218 that is then involved in a salt bridge with Asp451 (Figure 11).

Moving towards the docking pose of DADS that is situated outside the IIA binding pocket of HSA, several key interactions between the ligand and the protein. The interaction between one DADS SO_3^- function and Lys195, Lys199 and Arg218 are kept during the majority of the simulation while the second SO_3^- gets also involved with Lys195 most of the simulation and with Lys436 only at the beginning of the simulation (Figure 12). Lys195 bridging both sulfonate groups is therefore a key residue.

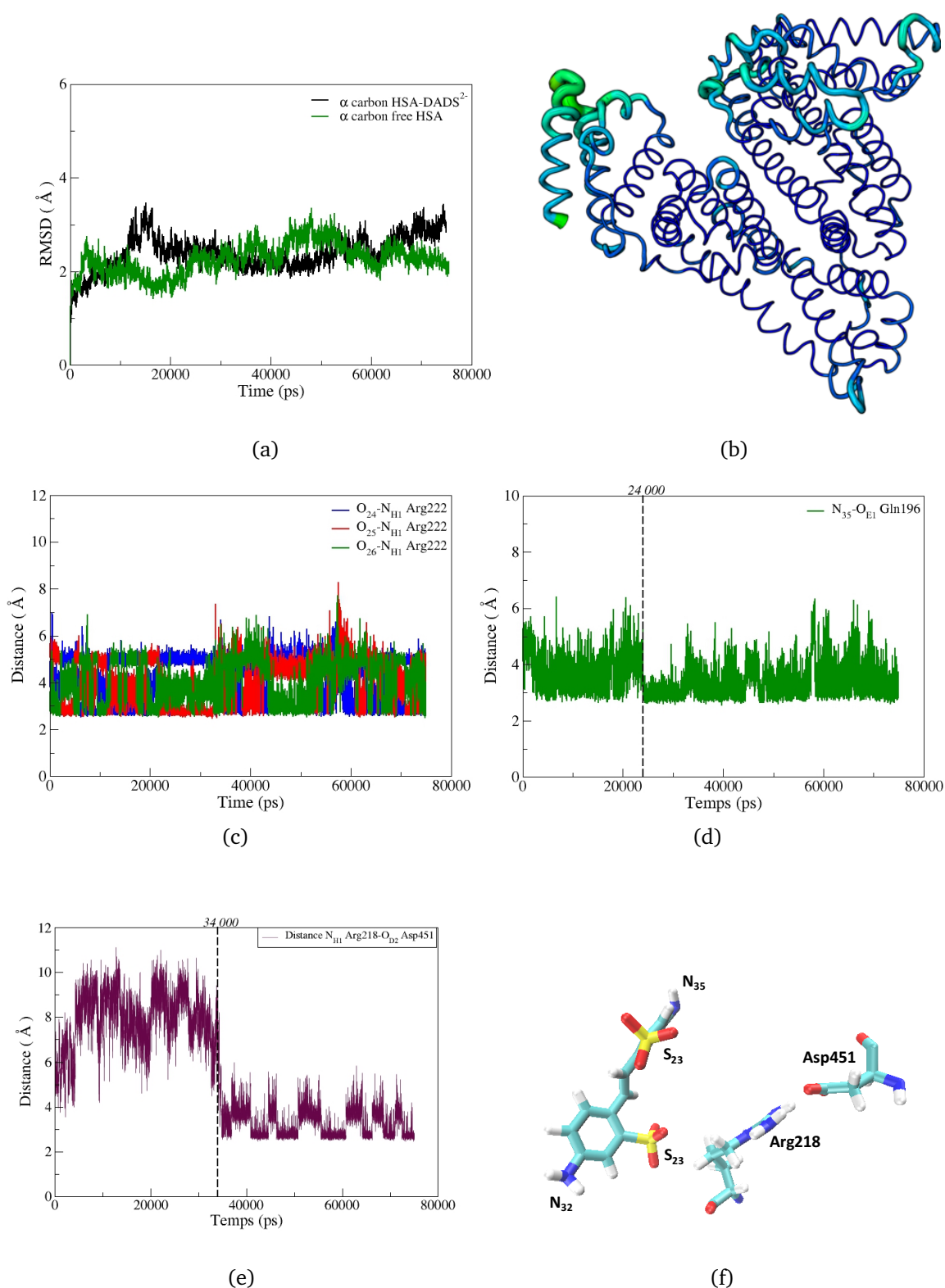


Figure ESI- 11 (a) RMSD of the apo (green) and holo (black) HSA protein. (b) RMSF for DADS embedded into IIA site (warfarin position) calculated from the 75 ns MD simulations; red and blue depict regions of higher and lower fluctuations, respectively. (c) Distance between the oxygen atoms of the sulfonate group and Arg222, (d) distance between N₃₅ of DADS and O of Gln196, (e) distance between the Arg218 terminal amino chemical group and the Asp451 carboxylate group of HSA obtained from the MD simulations. (f) Snapshots around 40 ns illustrating the presence of a salt-bridge between Arg218 and Asp451 extracted from the MD simulations.

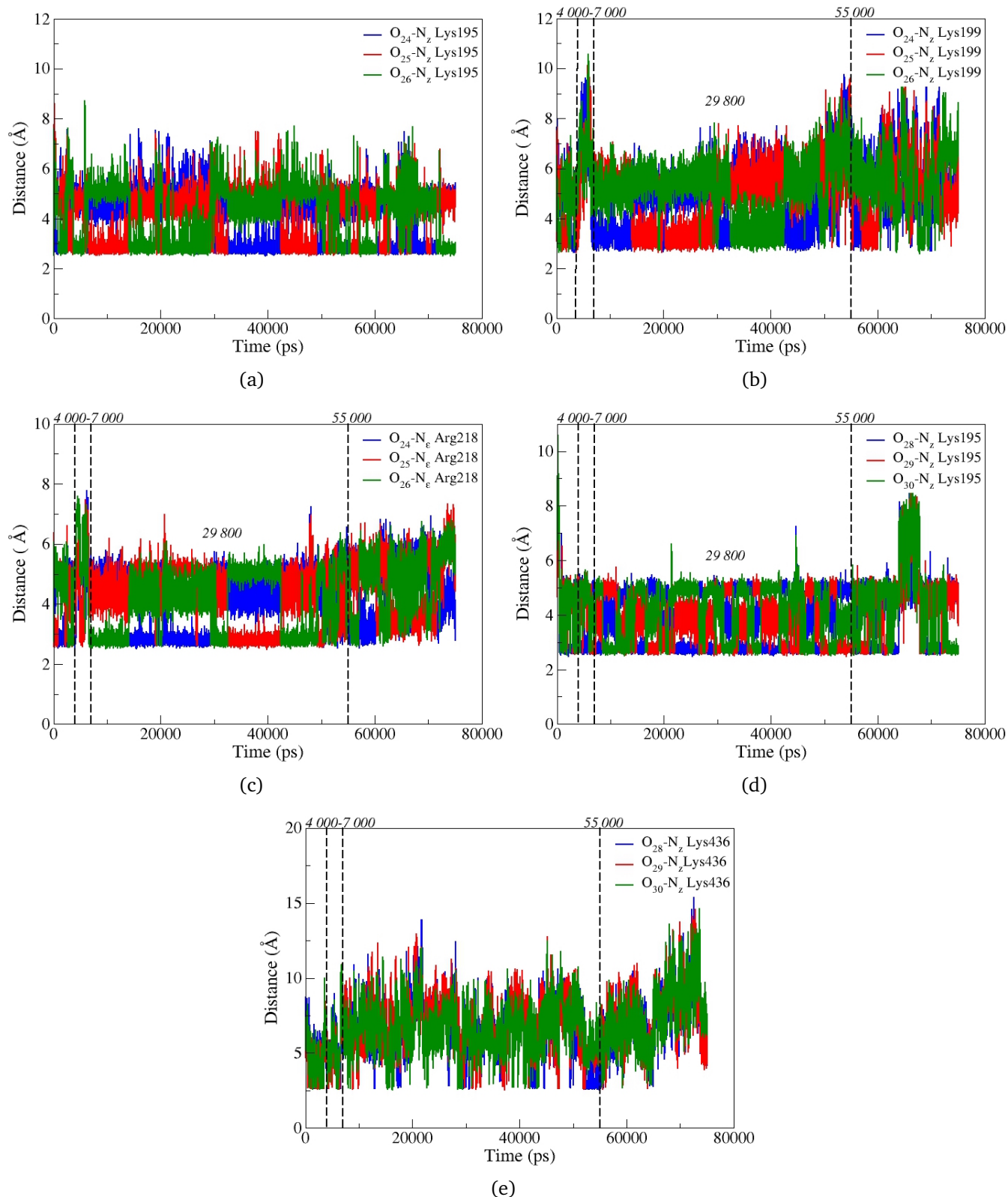
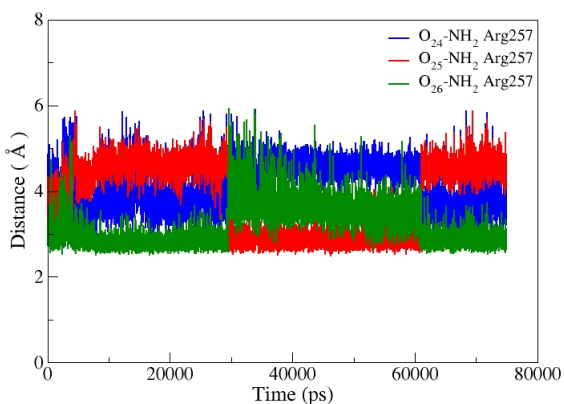
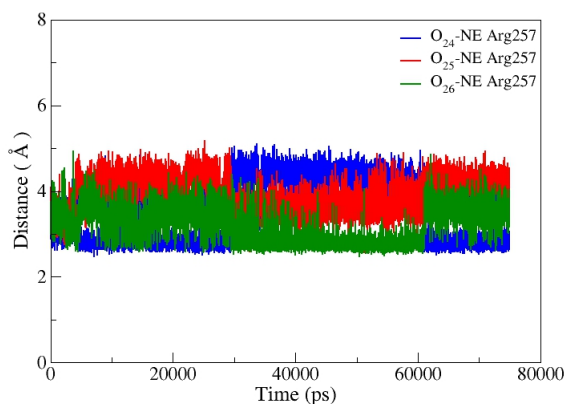


Figure ESI- 12 Distances between the oxygen atoms of the first DADS sulfonate group and (a) nitrogen of Lys195, (b) nitrogen of Lys199, (c) nitrogen of Arg218 of HSA obtained from the MD simulations. Distances between the oxygen atoms of the second DADS sulfonate group and (d) nitrogen of Lys195 and (e) nitrogen of Lys436 of HSA.

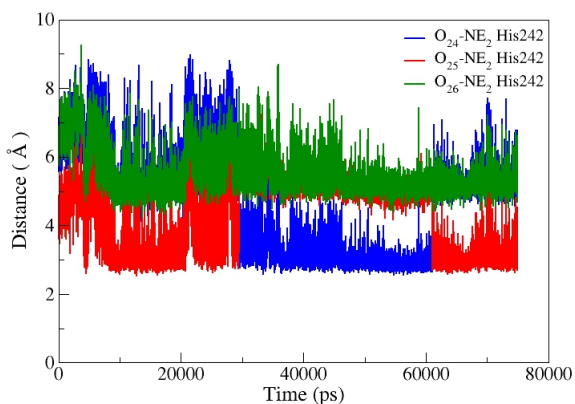
4.2 DNDS ligand



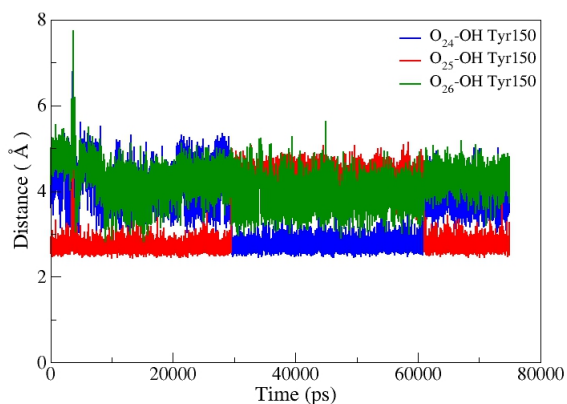
(a)



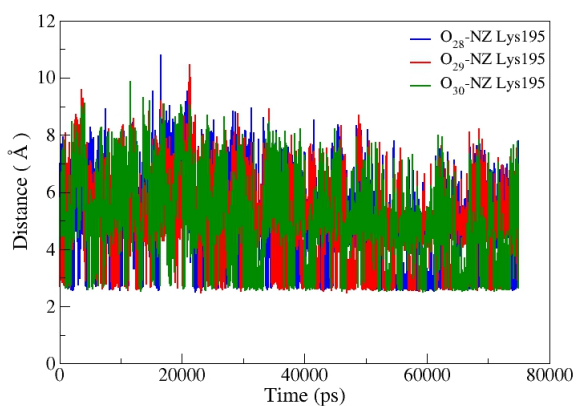
(b)



(c)



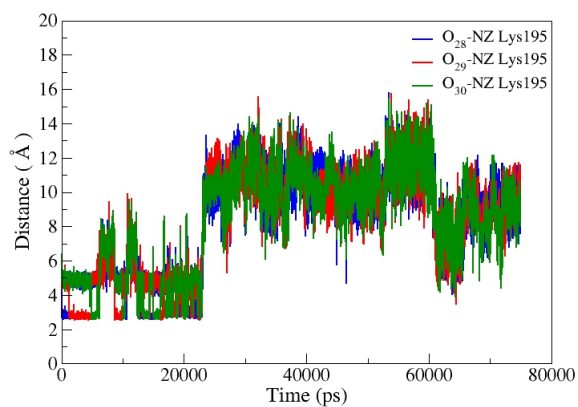
(d)



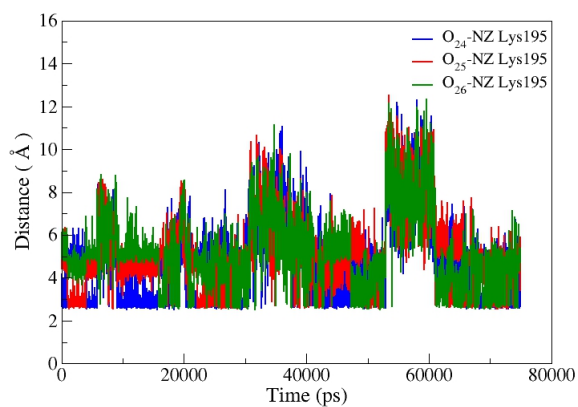
(e)

Figure ESI- 13 Distances between the oxygen atoms of the DNDS sulfonate groups and (a) backbone nitrogen of Arg257, (b) sidechain nitrogen of Arg257, (b) nitrogen of His242, (c) oxygen of Tyr150, (d) nitrogen of Lys195 of HSA obtained from the MD simulations.

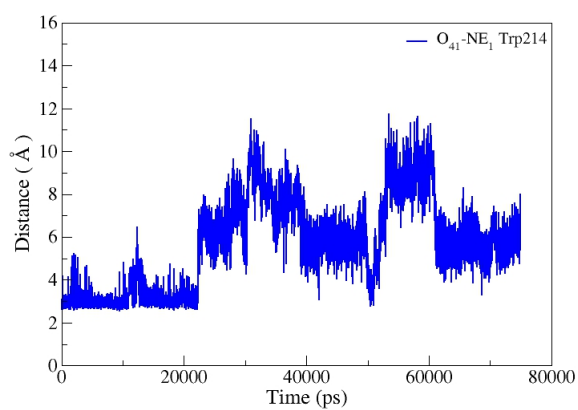
4.3 DATDS ligand



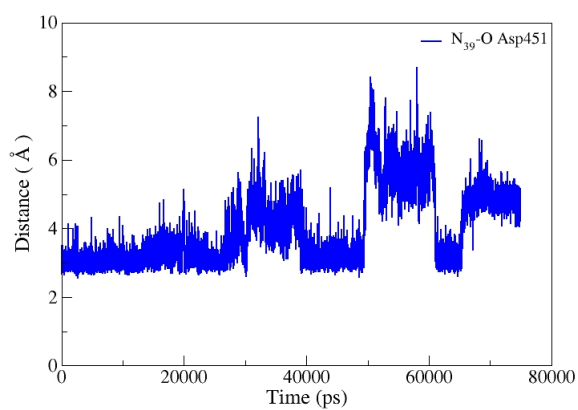
(a)



(b)



(c)



(d)

Figure ESI- 14 Distances between the oxygen atoms of the DATDS sulfonate groups and (a) and (b) nitrogen of Lys195, (c) nitrogen of Trp214, (d) sidechain nitrogen of Asp451 of HSA obtained from the MD simulations.

5 IIAIIB binding site

5.1 DADS ligand

The docking calculations of DADS generated 75 obtained poses dispersed in 8 clusters that are close to each other (less than 2.25 Å RMSD values, Figure 15). As for the other binding sites, the RMSF indicates that the presence of the DADS within the binding site does not significantly influence the global structure of HSA.

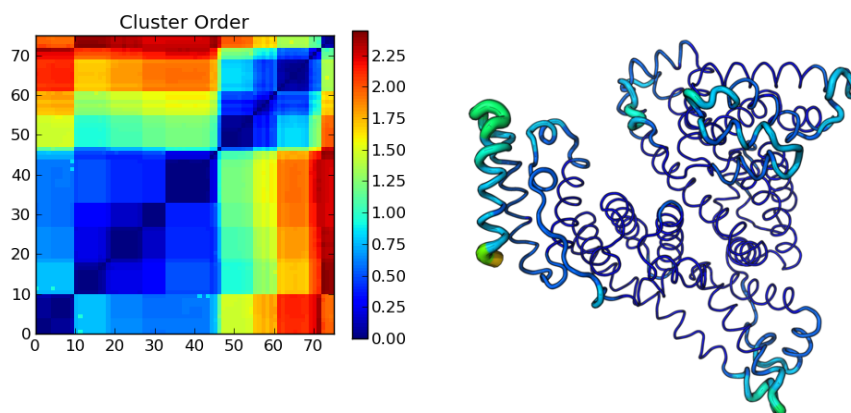


Figure ESI- 15 Left, RMSD matrix (Å) of the various DADS docking poses within the IIAIIB binding site of the HSA protein. Right, RMSF calculated from the 75 ns MD simulations; red and blue depict regions of higher and lower fluctuations, respectively.

5.2 DNDS ligand

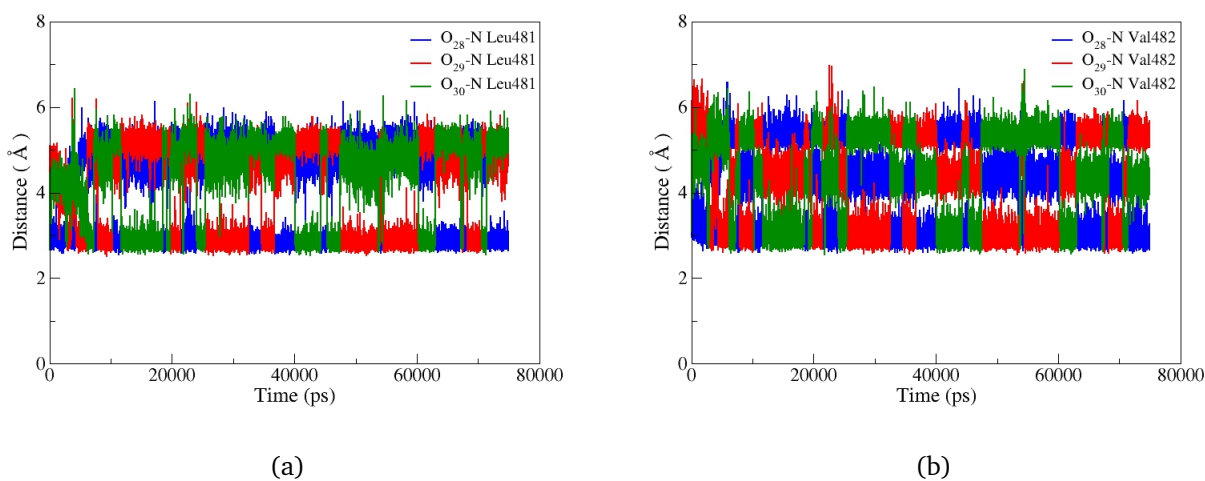
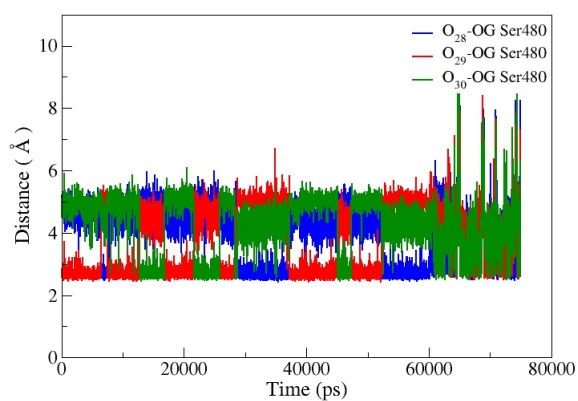
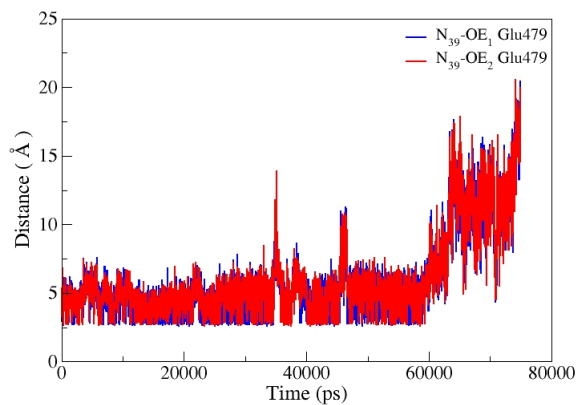


Figure ESI- 16 Distances between the oxygen atoms of the DNDS sulfonate groups and (a) backbone nitrogen of Leu481, (b) backbone nitrogen of Val482 of HSA obtained from the MD simulations.

5.3 DATDS ligand



(a)



(b)

Figure ESI- 17 Distances between the oxygen atoms of the DATDS sulfonate groups and (a) oxygen of Ser480, (b) sidechain oxygen atoms of Glu479 of HSA obtained from the MD simulations.

6 IIIA binding site

6.1 DADS ligand

The docking calculations of DADS generated 25 obtained poses dispersed in 4 clusters that are close to each other (less than 0.1 Å RMSD values, Figure 18).

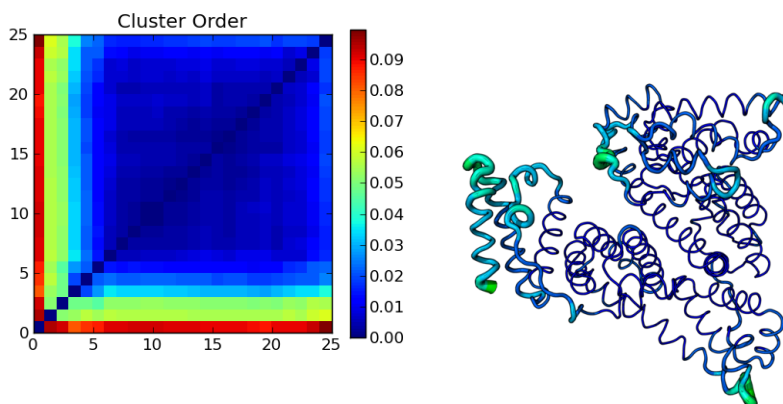


Figure ESI- 18 Left, RMSD matrix (Å) of the various DADS docking poses within the IIIA binding site of the HSA protein. Right, RMSF calculated from the 75 ns MD simulations; red and blue depict regions of higher and lower fluctuations, respectively.

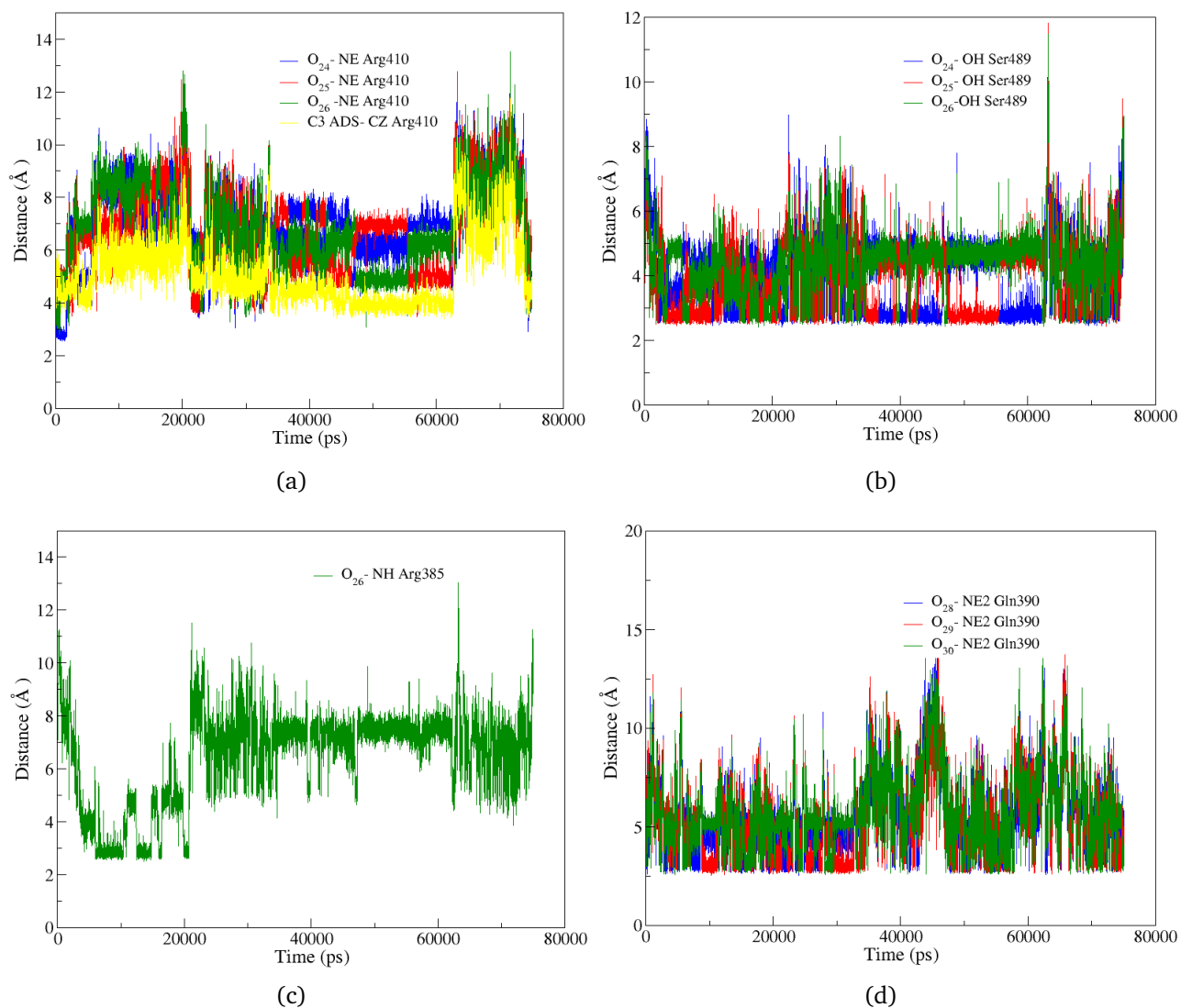


Figure ESI- 19 Distances between the oxygen atoms of the DADS sulfonate groups and (a) nitrogen of Arg410 , (b) oxygen of Ser489, (c) nitrogen of Arg385, (d) nitrogen of Gln390 of HSA obtained from the MD simulations.

6.2 DNDS ligand

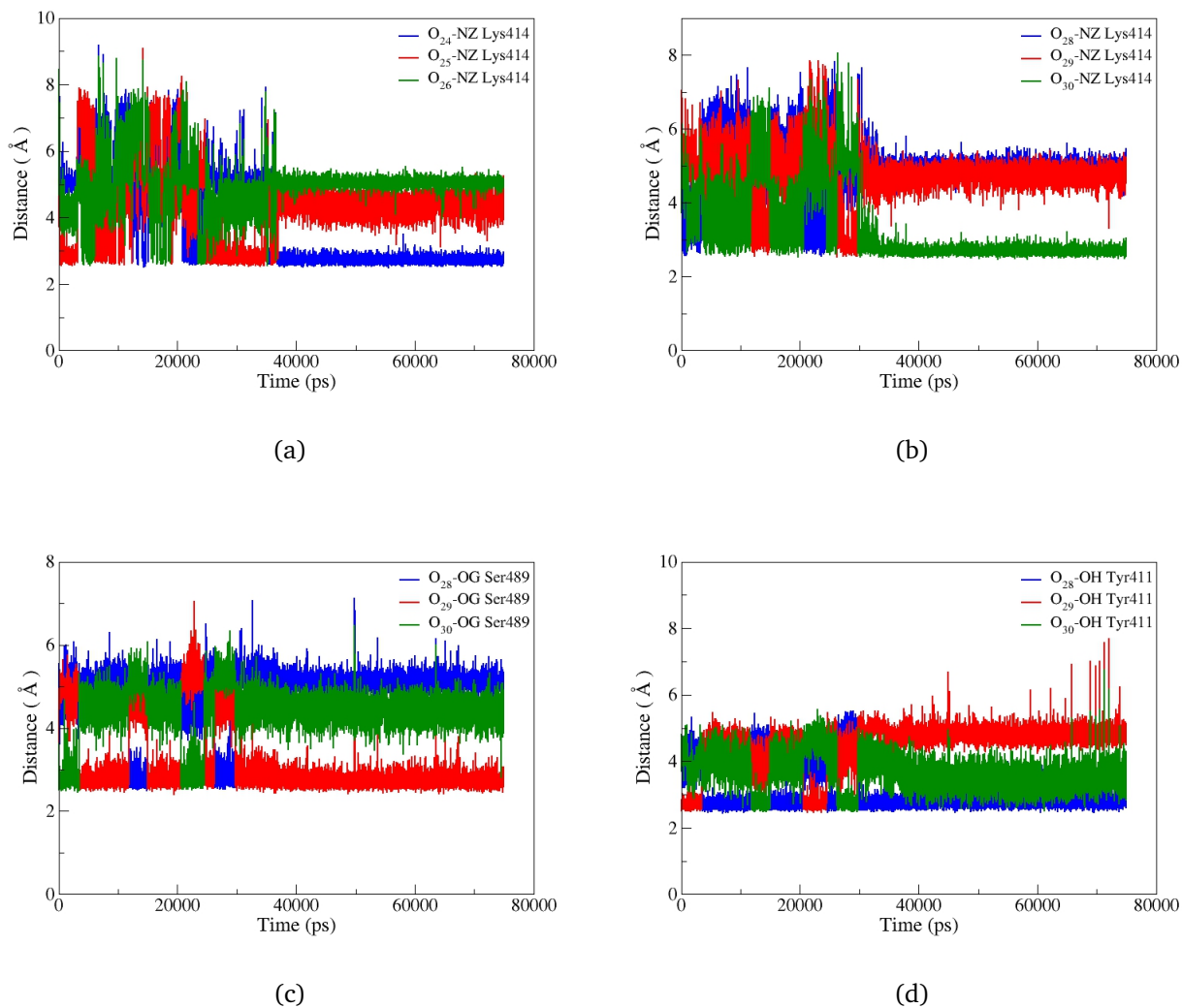
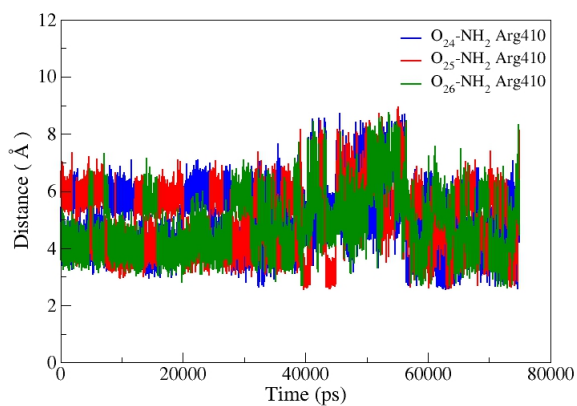
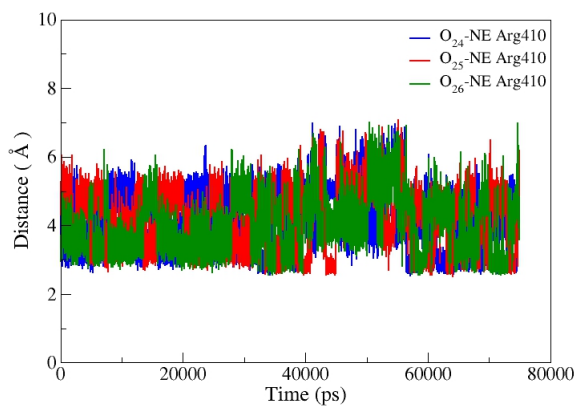


Figure ESI- 20 Distances between the oxygen atoms of the DNDS sulfonate groups and (a) and (b) nitrogen of Lys414, (c) oxygen of Ser489, (d) oxygen of Tyr411 of HSA obtained from the MD simulations.

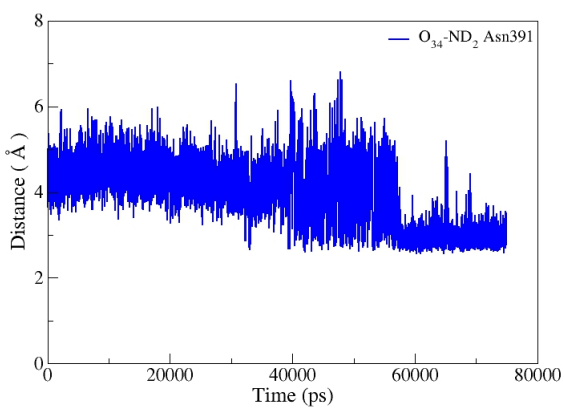
6.3 DATDS ligand



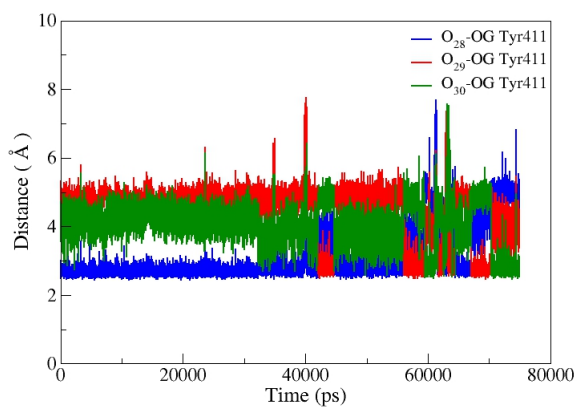
(a)



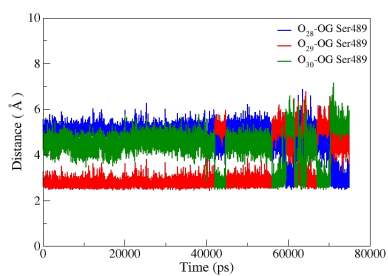
(b)



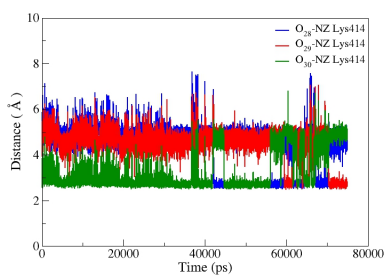
(c)



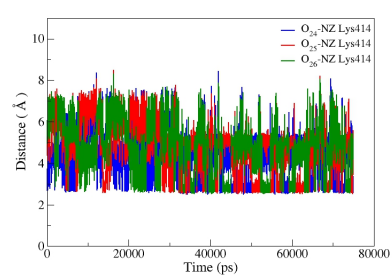
(d)



(e)



(f)



(g)

Figure ESI- 21 Distances between the oxygen atoms of the DATDS sulfonate groups and (a) and (b) backbone and sidechain nitrogen of Arg410, (c) As391, (d) oxygen atom of Tyr411, (e) sidechain oxygen atoms of Ser489, (f) and (g) nitrogen atom of Lys414 of HSA obtained from the MD simulations.

Notes and references

- [1] P. A. Zunszain, J. Ghuman, A. F. McDonagh and S. Curry, *J. Mol. Biol.*, 2008, **381**, 394–406.
- [2] J. Ghuman, P. A. Zunszain, I. Petitpas, A. A. Bhattacharya, M. Otagiri and S. Curry, *J. Mol. Biol.*, 2005, **353**, 38–52.